TOWARD HIGH-COVERAGE IMAGING OF HYDROTHERMAL VENT FIELDS: A RECURSIVE PATH-PLANNING METHOD OF AN AUV

Yoshiki Sato*, Toshihiro Maki*, Ayaka Kume, Takumi Matsuda**, Takashi Sakamaki*, and Tamaki Ura*****

*Institute of Industrial Science, The University of Tokyo
4-6-1, Komaba, Meguro-ku, Tokyo, 153-8505, Japan
**Graduate School of Frontier Sciences, The University of Tokyo
5-1-5, Kashiwanoha, Kashiwa-shi, Chiba, 277-8561, Japan
***Kyushu Institute of Technology
2-4, Hibikino, Wakamatsu-ku, Kitakyushu-shi, Fukuoka, 808-0196, Japan
{ys-sato, maki, kume, matsuda, sakamaki, ura}@iis.u-tokyo.ac.jp

Abstract

AUVs (Autonomous Underwater Vehicles) can operate without the need for human control nor tether cable as long as the energy persists. AUVs are recently used for seafloor imaging. However, AUVs cannot send observational results in detail to the surface during its operation. So it is impossible for operators to confirm in real time that there are no unobserved areas. If unobserved areas are found by post-processing, another deployment of the AUV is necessary to cover them, increasing the total cost.

A recursive observation method for an AUV had been proposed to realize a high coverage observation at one deployment. In the method, the AUV evaluates unobserved areas after the initial observation. If unobserved areas are found, the AUV creates the next path to cover them effectively. This paper reports the experimental results of the method at hydrothermal deposits at Kagoshima Bay in Japan. The AUV Tri-TON observed a chimney called Daifuku-yama. Although the AUV could not conduct the second observation as the computing time was too long, the AUV succeeded in creating a new path consisting of seven waypoints for the second observation of the chimney based on the initial observation. After the experiment, the 2D photomosaic and 3D image of the chimney was created in post-processing. An improvement in the method for unobserved area evaluation is also proposed to speed up calculation.

Introduction

Autonomous Underwater Vehicles (AUVs) have the advantage of being free from tether cables and human control. AUVs are recently used for seafloor imaging, as well as conventional acoustic survey. Visual observation by AUVs provides high-resolution color information of seafloor over a large area. For example, AUV Sirius was used to observe Great Barrier Reef [1], around Tasman Peninsula [2], Scott Reef [3] and so on. AUV Tri-Dog1 observed tube worm colonies at Tagiri vent field, Kagoshima Bay in Japan [4]. AUV DAGON, which is equipped with a GPU for image processing, was tested in the Baltic Sea [5]. As a conventional AUV follows a preplanned path, some part of the target is often left unobserved because of occlusions, positioning errors, and so on. If the unobserved areas were found after the deployment, an extra deployment is necessary to cover them, increasing the total cost.

A recursive observation method based on on-site path re-planning has been proposed with basic verification through tank experiments [6] and real sea experiments [7]. In the method, the AUV evaluates unobserved area and creates the next path to cover them effectively. In this paper, the outline of the proposed method is described and the experimental result at hydrothermal deposits is reported. Moreover, the feasibility of high-coverage imaging of hydrothermal vent fields by proposed method is discussed.

Outline of the Path Re-planning Method

This chapter explains the outline of the proposed method. Details are described in the previous report [6]. The proposed method requires an AUV that satisfies the following three conditions:

1) The AUV is hovering type,
2) The AUV has the ability of obstacle avoidance and self-localization with accuracy enough for the purpose of the survey,
3) The AUV has at least one camera and terrain measuring sensor to evaluate unobserved areas.

The concept of the method is illustrated in Fig. 1. At first, the AUV observes the seafloor according to a preplanned path (I. Initial observation phase). Secondly, the AUV stands and estimates unobserved area on-site based on the data obtained in the initial observation (II. Calculation phase). Then the AUV makes a 3D bathymetry map and detects unobserved areas from the map. If unobserved areas were found, the AUV creates new path to observe them effectively. The AUV then follows the new path (III. Re-observation phase). Finally, the full coverage 3D image map is obtained by post-processing.

In the initial observation, the AUV obtains point cloud representing the terrain. An example of the point could is shown in Fig. 2. The example data was obtained in the experiment at Suruga Bay in Japan in November 2012 [7]. In the experiment, an artificial target was set up on the seafloor and the AUV Tri-TON [8] measured bathymetry using the light-section ranging system [9]. The lack of measurements is due to the environment. As the water was murky, the laser footprints captured by cameras were too weak. To eliminate outliers, the denoising process is executed at the beginning of the calculation phase. The terrain measurements those have less than *n* other measurements within the distance *d* were excluded as outliers. Here, *n* and *d* are constant. The terrain measurement after denoising is shown in Fig. 3. Then, 3D triangulated mesh is constructed by Delanuay triangulation [10] as in Fig. 4. Each cell of the mesh is evaluated according to the procedure shown in Fig. 5 in order to find unobserved areas. The procedure consists of the four constraints: I) the distance, II) the angle of view, III) the angle offset and IV) the obstacle. The unobserved area estimated in the calculation phase is shown in Fig. 6. The green and blue regions were judged to be covered. The red regions were judged to be unobserved.

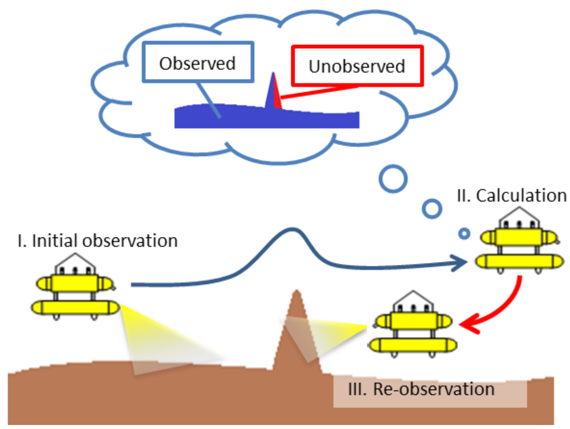

Fig. 1 Concept of the proposed method.

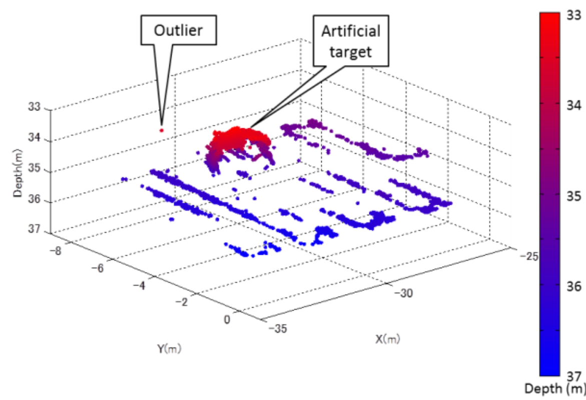

Fig. 2 An example of obtained point cloud representing the terrain.

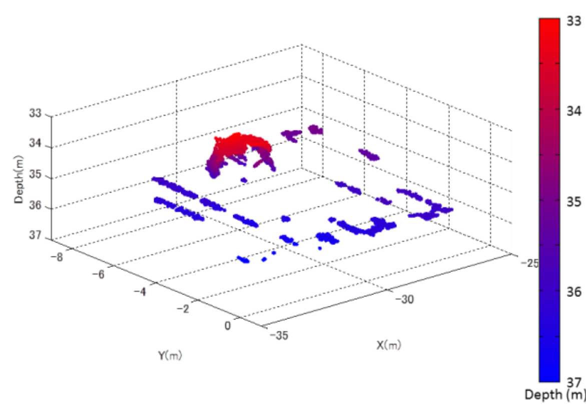

Fig. 3 The results of denoising.

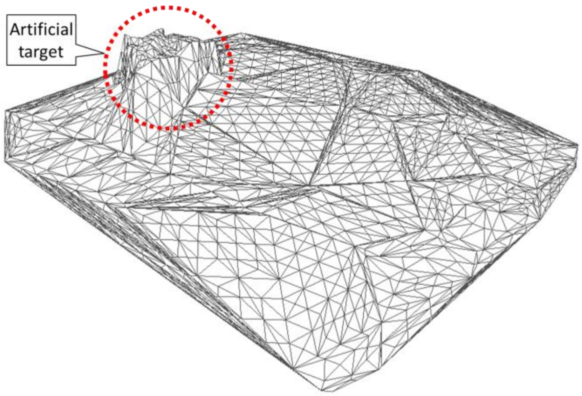

Fig. 4 3D triangulated mesh.

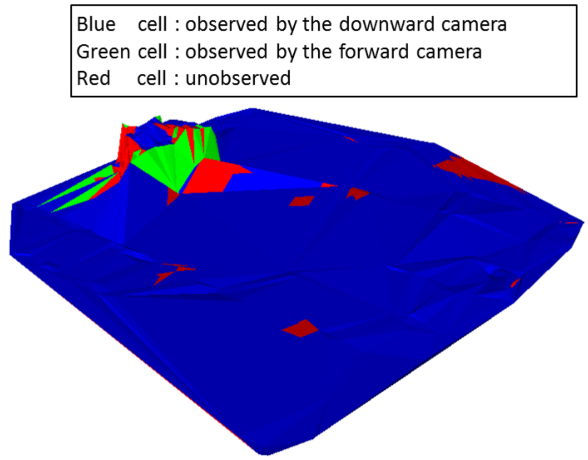

Fig. 6 Result of mesh evaluation.

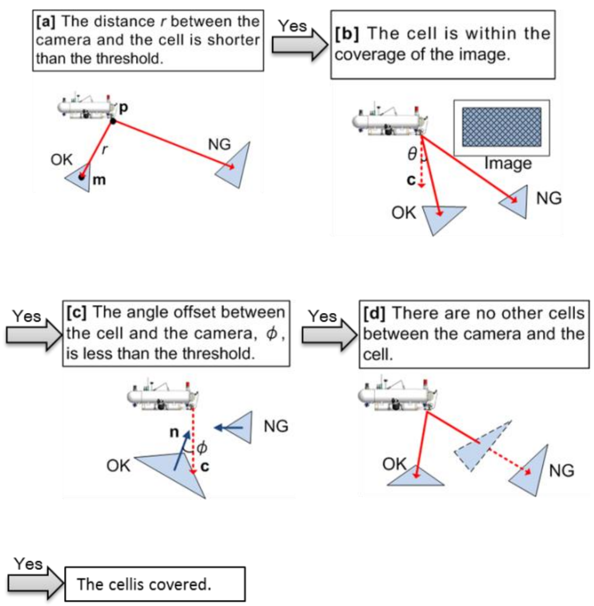

Fig. 5 Mesh evaluation procedure.

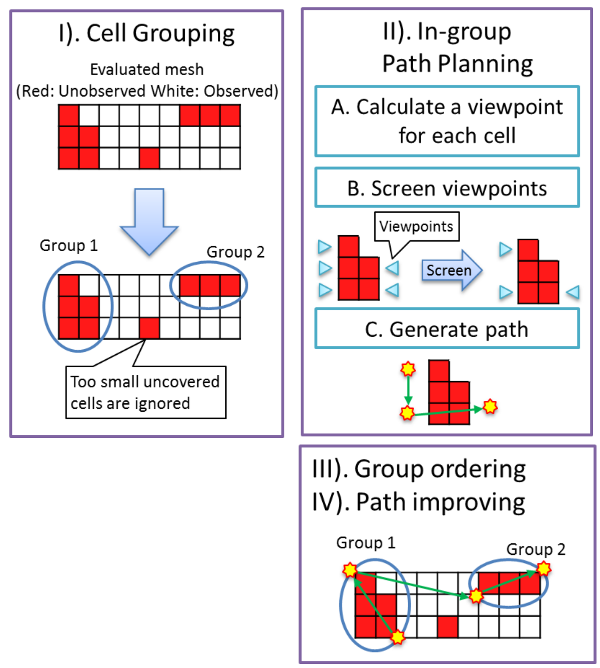

Fig. 7 Outline of path planning.

After the mesh evaluation, the AUV creates new path to observe the unobserved cell as illustrated in Fig. 7. In order to complete the process in a realistic time, the method generates not an optimized solution but an executable one. The path planning method consists of the four steps:

I). All of the uncovered cells are split into groups by their positions. However, too small cells are ignored.

II). The path is generated for each group by calculating a view point for each cell.

III). The order of the groups is decided.

IV). The path is improved by changing the order of the waypoints.

Auv Tri-TON

The proposed method was implemented to the hovering type AUV Tri-TON [8]. The AUV was developed by Institute of Industrial Science, the University of Tokyo in 2011. The AUV was constructed as a test bed under the governmental project to develop instruments to estimate ore reserves in underwater hydrothermal deposits. The main specifications and overview are shown in Table

1 and Fig. 8, respectively. The AUV can move in surge, sway, and heave direction and make a pivot turn by using five thrusters. The AUV uses a Doppler Velocity Log (DVL), a Fiber Optic Gyro (FOG), and the ALOC (Acoustic LOcalization and Communication device, which is a SBL based acoustic positioning and communication device) to stochastically estimate its position and orientation based on a seafloor station shown in Fig. 9 [11,12]. The station is equipped with a depth sensor, digital compass and ALOC.

In order to measure bathymetry, the AUV has two light-section ranging systems as shown in Fig. 10. The light-section ranging system consists of a camera and a sheet laser [9]. In Fig. 10, the blue lines and green lines show the field of view of the cameras and the traces of the sheet lasers, respectively. During seafloor observations, the AUV takes images every second at a velocity of 0.08 m/s. The AUV uses flash once in every 10 shots to obtain an illuminated color image. The remaining images are taken with the sheet laser to obtain bathymetry.

Table 1. Main specifications of Tri-TON.

Vehicle	
Size	1.40 m (L) x 1.33 m (H) x 0.76 m (W)
Mass	230 kg
Max. speed	0.5 m/s
Max. depth	800 m
Thruster	100 W x 5 Surge x 2, Sway x 1, Heave x 2
Battery	Li-Ion 26.6 V 25 Ah x 4
Communication	Wi-Fi (in air), ALOC (underwater)
CPU	Intel Atom Z530 x 2 (Main & Vision)
OS	Microsoft WindowsXP
Navigational Instruments	
Ground velocity	Teledyne RDI Navigator (DVL)
Depth	Mensor DPT6000
Roll & Pitch	OceanServer OS5000
Heading rate	JAE JG-35FD (FOG)
Obstacle search	Tritech Micron (Scanning sonar)
Position	GPS (in air), ALOC (underwater)
Imaging Instruments	
Flash	Morris Hikaru-komachi 6 x 2
Sheet laser	Global laser GreenLyte-MV Excel x 2
Camera	Lumenera Lm165 x 2

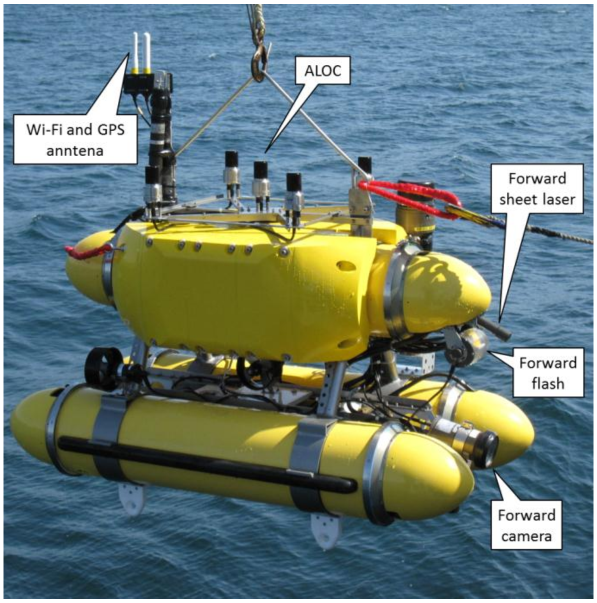

Fig. 8 AUV Tri-TON.

Fig. 9 Seafloor station.

Experiments at hydrothermal deposits

The sea experiments were held at hydrothermal deposits at Kagoshima Bay in Japan, in December 2012. The depth of the site was around 200 m. The aim of the experiments is to confirm the validity of the proposed method in rough terrain area.

At first, the seafloor station was placed at about 30 m away from the hydrothermal chimney, known as Daifuku-yama. The station serves as the positional reference for the AUV Tri-TON. Secondly, the AUV was deployed. After reaching the seafloor, the AUV searched for the station by ALOC while following the predetermined hexagonal path indicated by the blue line in Fig. 11. The radius of the hexagon was 60 m. The AUV stopped the search when the station was found. The AUV spent about 24 minutes to find the station. The estimated position and direction of the station are shown in Fig. 11 as the star and the bar, respectively. Thirdly, the AUV performed the initial observation. In the initial observation phase, the AUV observed around the estimated chimney area in about 35 minutes according to the pre-determined path as indicated by the magenta line in Fig. 11. After the initial observation, The AUV entered the calculation phase. However, the AUV could not perform the re-observation as the AUV ran out of time before finishing the calculation.

Fig. 12 shows the measured depth and altitude of the AUV during the deployment. The origin of the elapsed time is the beginning of searching the station. The reference altitude of the AUV was 1.6 m. The phase of the AUV is shown in the top of the figure. The rapid change in depth during the initial observation indicates that the AUV passed rough terrain, as the AUV kept constant altitude. Fig. 13 shows the measurement and reference of surge velocity. At the first term, the reference is relatively fast (which is 0.12 m/s) because the AUV must explore wide area to finding the station. After finding the station, the AUV takes images every second at a velocity of 0.08 m/s. Figs 14 and 15 are the standard deviations of estimation error of position and heading, respectively.

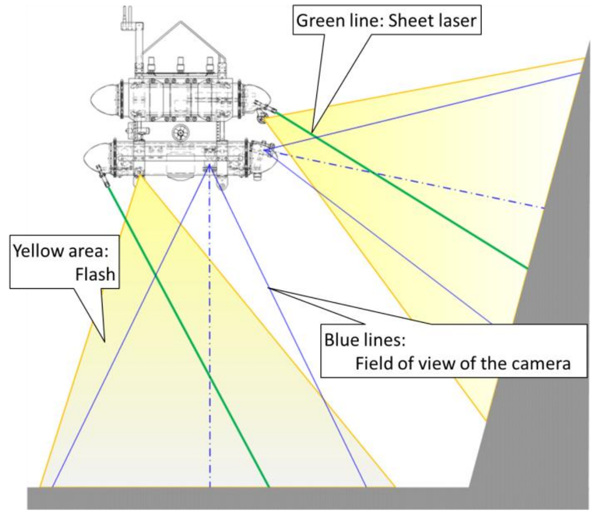

Fig. 10 Imaging instruments of Tri-TON.

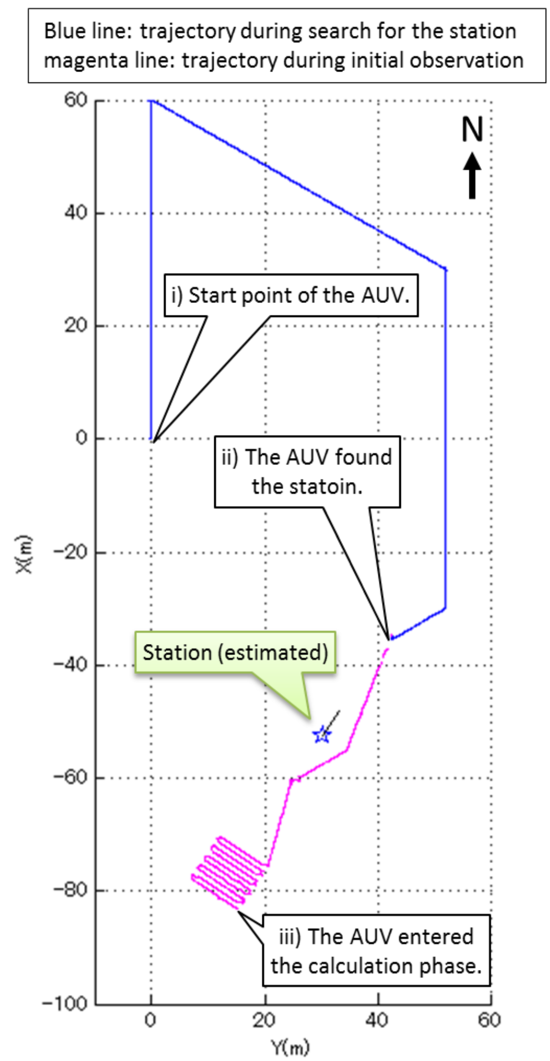

Fig. 11 The trajectory of Tri-TON.

Finally, the obtained point cloud representing the terrain is shown in blue dot in Fig. 16. In Fig. 16, the magenta line shows the trajectory of the AUV. The uplift on the terrain is the Daifuku-yama chimney. The high resolution 2D photomosaic of the seafloor shown in Fig. 17 was yielded by post processing. Moreover, the high resolution 3D image reconstruction shown in Fig. 18 was obtained by combining the point cloud with the photomosaic.

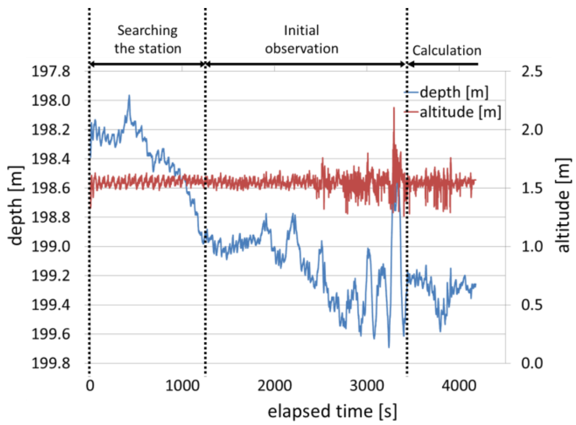

Fig. 12 Depth and altitude of the AUV.

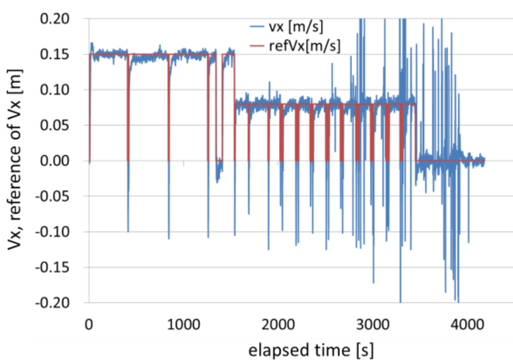

Fig. 13 Surge velocity of the AUV.

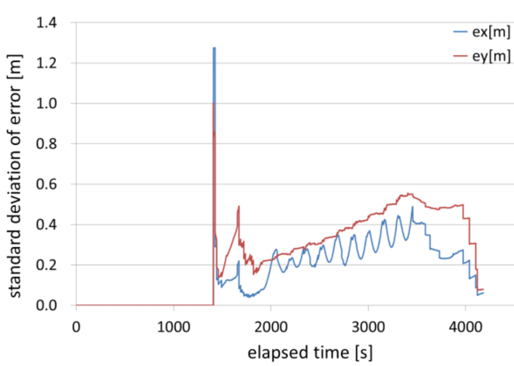

Fig. 14 Standard deviation of position estimation error.

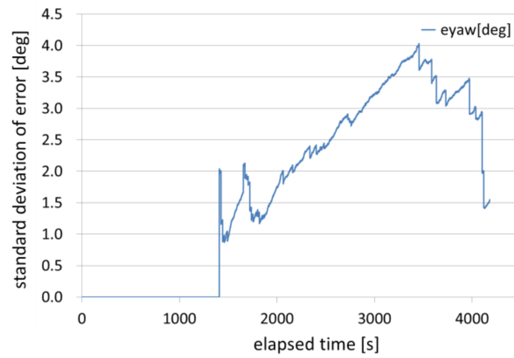

Fig. 15 Standard deviation of heading estimation error.

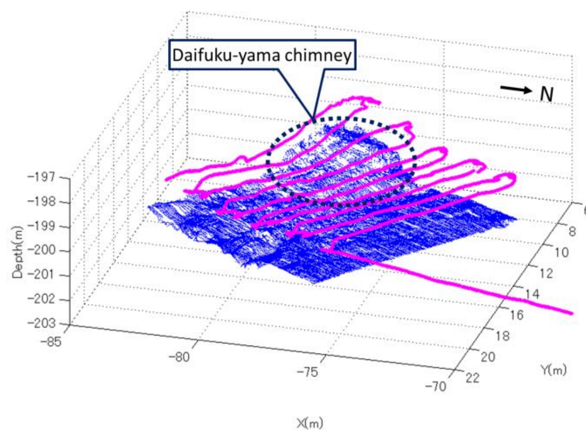

Fig. 16 Obtained point cloud representing the terrain.

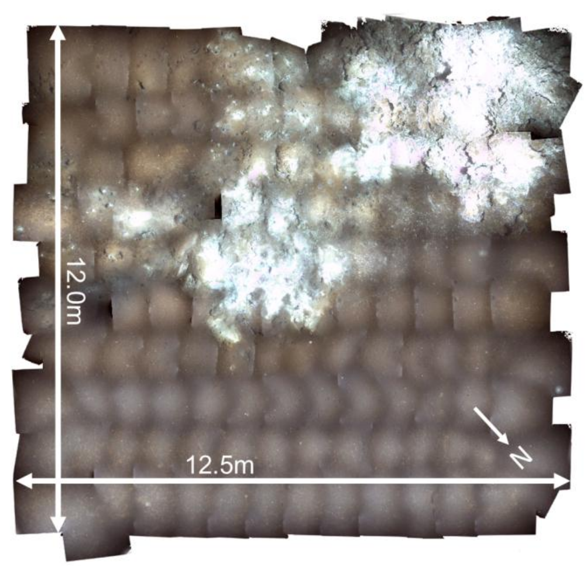

Fig. 17 Large scale photomosaic obtained by post processing.

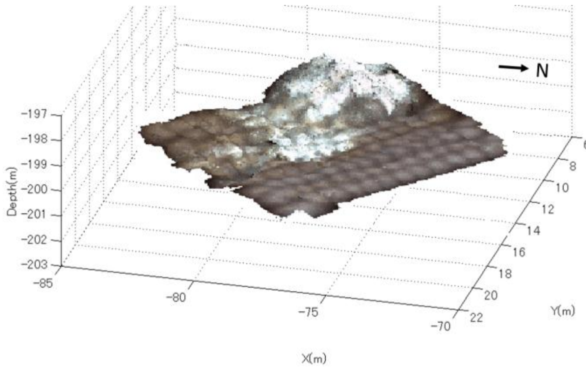

Fig. 18 3D image reconstruction.

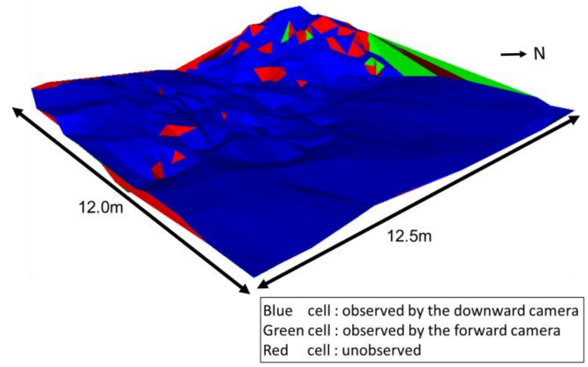

Fig. 19 Results of mesh evaluation.

The feasibility of the method in hydrothermal vent field

In the experiment, the AUV could not finish the calculation within the assigned time. Therefore, the result of bathymetry mesh evaluation shown in Fig. 19 was obtained after the experiment. The green and blue regions were judged to be covered by the forward and downward camera, respectively. The red regions were judged to be unobserved. Fig. 19 shows that the red cells are concentrated in the uplift part. After the mesh evaluation, the new path consisting of seven waypoints for the re-observation was created. Table 2 shows the new waypoints. When the downward camera was used, the AUV can head to any direction because its view is not affected by the heading of the AUV. The new path is indicated in green line in Fig. 20. The magenta line shows the trajectory of the AUV at the initial observation. The bracketed numbers correspond to the waypoint numbers in Table 2. The waypoints 5, 6 and 7 were generated on the chimney, where many unobserved areas were found. Therefore, the AUV succeeded to generate a new path for the re-observation. As a result, the proposed method has feasibility of high-coverage imaging of hydrothermal vent fields.

However, when there are many unobserved areas, time reduction of the calculation phase is required. Actually, most of the computational resource was dedicated to the denoising process at the experiment. Therefore, optimization of the denoising algorithm is important. The denoising algorithm is shown in Algorithm 1.

Table 2. The new waypoints obtained at the calculation phase.

Waypoint No.	Camera	X [m]	Y [m]	Depth [m]	Heading [deg]
(1)	Downward	-27.42	4.68	200.57	- -
(2)	Downward	-28.63	4.67	200.81	- -
(3)	Downward	-34.84	2.44	199.29	- -
(4)	Downward	-34.67	1.34	201.11	- -
(5)	Downward	-34.66	-1.70	200.74	- -
(6)	Downward	-32.28	-0.77	200.94	- -
(7)	Downward	-29.47	-4.69	200.92	- -

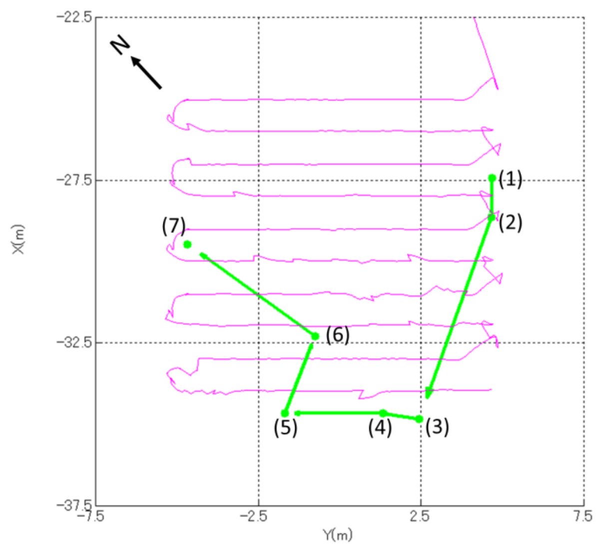

Fig. 20 The AUV's new path for the re-observation phase.

Algorithm 1. Denoising process

```
for i = 0 to N-1 do
  count = 0;
  for j = 0 to N-1 do
    if (i = j) then
      continue;
    end if
    if ( dist(x_i, x_j) <= d ) then
      count = count + 1;
    end if
    if ( count >= n ) then
      x_i is valid;
    end if
  end for
end for
```

In the Algorithm 1, the *i*, *j*, *N*, *count*, $dist(x_i, x_j)$ represent the iteration variable for the outer loop, variable for the inner loop, total number of the point cloud data, local counter, distance between the *i*-th point cloud data with *j*-th point cloud data, respectively. Since the algorithm calculates the distance in brute force, the required cost can be $O(N^2/2)$ order in average. Since the point cloud data will be obtained according to the movement of the AUV, the spacial locality and temporal locality are available. The usage of the locality of reference is effective to the ordinary processor employed the harvard architecture. To use the locality of reference, Algorithm 1 was replaced by the Algorithm 2. The Algorithm 2 introduces the variable *offset* to the *i*-th data instead of the iteration variable *j*. So that the data close to the *i*-th data have a priority to refer, cost reduction can be expected.

The Algorithm 2 achieved 1296.1 times of speedup ratio to the cloud data in Fig. 16. Although applying 98 minutes in the calculation is unrealistic, the optimization can reduce to less than a minute. So the proposed method is applicative enough.

Algorithm 2. Optimized denoising process

```
for i = 0 to N-1 do
  count = 0;
  for offset = 1 to N-1 do
    if (i + offset < N) then
      if ( dist(x_i, x_{i+offset}) <= d ) then
        count = count + 1;
      end if
    end if
    if (i - offset >=0) then
      if ( dist(x_i, x_{i-offset}) <= d ) then
        count = count + 1;
      end if
    end if
    if ( count >= n ) then
      x_i is valid;
    end if
  end for
end for
```

Conclusion

In this paper, the path re-planning method, that can cover unobserved area at one dive, was examined in real hydrothermal deposits. The AUV Tri-TON was deployed to observe a hydrothermal chimney. As the result of validation after the experiment, it was confirmed that the AUV succeeded to generate a new path for re-observe the chimney. In order to realize the proposed method, optimizing of the denoising process was required. Therefore, the optimized denoising algorithm that focuses on locality of reference was introduced in this paper. After the optimization, the denoising process achieved 1296.1 times of speedup ratio. The optimization can yield feasibility of the method in hydrothermal vent field.

Acknowledgment

This work is supported by the Ministry of Education, Cultule, Sports, Science and Technology (MEXT) of Japan. The experiments were held during the cruise of Nansei-maru, Kagoshima University. The authors thank T. Yamamoto, associate professor of Kagoshima University, and all the crew of the Nansei-maru for their support.

References

[1] M. J. Roberson, O. Pizarro, S. B. Williams and I. Mahon, "Generation and visualization of large-scale three-dimensional reconstructions from underwater robotic surveys," *Journal of Field Robotics*, Vol.27, No.1, pp.21-51, 2010.

[2] M. J. Stefan, B. Williams, O. Pizarro and N. Barrett, "AUV Benthic Habitat Mapping in South Eastern Tasmania," *Field and Service Robotics, Springer Tracts in Advanced Robotics*, Vol.62, pp.275-284, 2010.

[3] A. Friedman, O. Pizarro, S. B. Williams and M. J. Roberson, "Multi-Scale Measures of Rugosity, Slope and Aspect from Benthic Stereo Image Reconstructions," *PloS* ONE, No.12, 2012.

[4] T. Maki, A. Kume and T. Ura, "Volumetric mapping of tubeworm colinies in Kagoshima Bay through autonomous robotic surveys," *Deep Sea Research Part I: Oceanographic Research Papers*, Vol.58, No.7, 2011.

[5] M. Hildebrandt, C. Gaudig, L. Christensen, S. Natarajan, P. Paranhos and J. Albiez, "Two years of Experiments with the AUV Dagon – a Versatile Vehicle for High Precision Visual Mapping and Algorithm Evaluation," *Proceedings of IEEE/OES Autonomous Underwater Vehicles*, pp.1-9, 2012.

[6] A. Kume, T. Maki, T. Sakamaki, T. Ura, "Path re-planning method for an AUV to image rough terrain by on-site quality evaluation," *IEEE OCEANS'12 Yeosu*, pp.1-9, 2012.

[7] Y. Sato, T. Maki, A. Kume, T. Matsuda, T. Sakamaki, T. Ura, "Field Experimental Results of Path Re-planning Method for an AUV to Visualize Complicated Surface in 3D," *proceedings of The Underwater Technology UT'13*, UT2013-1122, 2013.

[8] T. Maki, T. Matsuda, A. Kume, Y. Sato, T. Sakamaki, T. Ura, "Development of the AUV Tri-TON for Imaging Rough Seafloor," In *The 23rd Ocean Engineering Symposium*, 2012. (in Japanese)

[9] H. Kondo, T. Maki, T. Ura, Y. Nose, T. Sakamaki, M. Inaishi, "Structure tracing with a ranging system using a sheet laser beam," *Proceedings of Underwater Technology UT'04*, pp.83-88, 2004.

[10] M. Gross and H. Pfster, editors. "Point-Based Graphics," *Morgan Kaufmann*, 2007.

[11] T. Maki, T. Matsuda, T. Sakamaki, T. Ura, "AUV navigation with a single seafloor station based on mutual orientation measurements," *Proceedings of Underwater Technology UT'11, pp.1-7, 2011*.

[12] H. Kondo, T. Maki, T. Ura and T. Sakamaki, "AUV NAVIGATION BASED ON MULTI-SENSOR FUSION FOR BREAKWATER OBSERVATION," *Proceedings of The 23rd International Symposium on Automation and Robotics in Construction 2006*, pp.72-77, 2006.